

DOUBLE FLIP MOVE FOR ISING MODELS WITH MIXED BOUNDARY CONDITIONS*

Lexing Ying¹⁾

Department of Mathematics, Stanford University, Stanford, CA 94305, USA

Email: lexing@stanford.edu

Abstract

This note introduces the double flip move to accelerate the Swendsen-Wang algorithm for Ising models with mixed boundary conditions below the critical temperature. The double flip move consists of a geometric flip of the spin lattice followed by a spin value flip. Both symmetric and approximately symmetric models are considered. We prove the detailed balance of the double flip move and demonstrate its empirical efficiency in mixing.

Mathematics subject classification: 82B20, 82B80.

Key words: Ising model, Mixed boundary condition, Swendsen-Wang algorithm.

1. Introduction

This note is concerned with the Monte Carlo sampling of Ising models with mixed boundary conditions. Consider a graph $G = (V, E)$ with the vertex set V and the edge set E . Assume that $V = I \cup B$, where I is the subset of interior vertices and B the subset of boundary vertices. Throughout the note, we use i, j to denote the vertices in I and b for the vertices in B . For the edges, we use $e = ij \in E$ to denote an interior edge between two interior vertices i and j , and $e = ib \in E$ for an interior-boundary edge between interior vertex i and boundary vertex b . The boundary condition is specified by $f = (f_b)_{b \in B}$.

A spin configuration $s = (s_i)_{i \in I}$ over the interior vertex set I is an assignment of ± 1 value to each vertex $i \in I$. The energy of the spin configuration s is given by the Hamiltonian function

$$H(s) = - \sum_{ij \in E} s_i s_j - \sum_{ib \in E} s_i f_b.$$

At a physical temperature T , the configuration probability of $s = (s_i)_{i \in I}$ is given by the Gibbs or Boltzmann distribution

$$p_I(s) = \frac{e^{-\beta H(s)}}{Z_\beta} \sim \exp \left(\beta \sum_{ij \in E} s_i s_j + \beta \sum_{ib \in E} s_i f_b \right), \quad (1.1)$$

where $\beta = 1/T$ is the inverse temperature and $Z_\beta = \sum_s e^{-\beta H(s)}$ is the renormalization constant (or the partition function).

One key feature of these models is that, below the critical temperature and under certain boundary conditions, the Gibbs distribution exhibits macroscopically different profiles. Fig. 1.1 provides two such examples, where black denotes $+1$ and yellow denotes -1 . In Fig. 1.1(a),

* Received August 10, 2022 / Revised version received September 6, 2022 / Accepted November, 28, 2022 /
Published online xx xx, 2023 /

¹⁾ Corresponding author

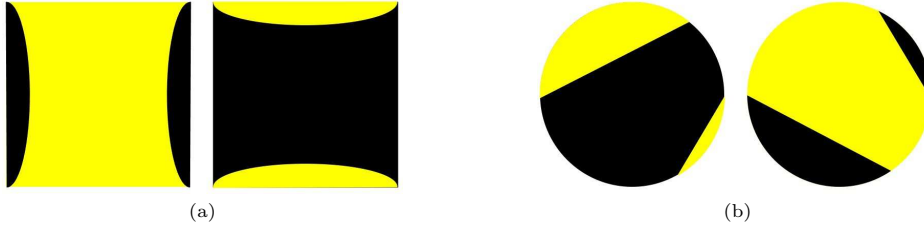


Fig. 1.1. Ising models with mixed boundary condition. (a) a square lattice and (b) a triangular lattice support on a disk. In each example, the model exhibits two macroscopically different profiles.

the square Ising lattice has the $+1$ condition on the two vertical sides but the -1 condition on the two horizontal sides. There are two macroscopic profiles: one contains a dominant -1 cluster linking two horizontal sides and the other contains a dominant $+1$ cluster linking two vertical sides. In Fig. 1.1(b), the Ising lattice supported on a disk has the $+1$ condition on two disjoint arcs and the -1 condition on the other two. This model also exhibits two macroscopically different profiles shown in Fig. 1.1(b). Notice that in each example, due to the symmetry or approximate symmetry of the Ising lattice as well as the boundary condition, the two macroscopic profiles have comparable probabilities. Therefore, any effective sampling algorithm is required to visit both profiles frequently.

One of the most well-known methods for sampling Ising models is the Swendsen-Wang algorithm [9], which iterates between the following two substeps in each iteration:

1. Given the current spin configuration, generate an edge configuration according the inverse temperature β (see Section 2 for details).
2. To each connected component (also called cluster) of the edge configuration, assign to all spins in this cluster all $+1$ or -1 to with equal probability. This results in a new spin configuration.

For many boundary conditions including the free boundary condition, the Swendsen-Wang algorithm exhibits rapid mixing for all temperatures. However, for the mixed boundary conditions shown in Fig. 1.1, the Swendsen-Wang algorithm experiences slow convergence under the critical temperatures, i.e., $T < T_c$ or equivalently $\beta > \beta_c$. The reason is that, for such a boundary condition, the energy barrier between the two macroscopic profiles is much higher than the typical energy fluctuation. In other words, the Swendsen-Wang algorithm needs to break a macroscopic number of edges between aligned adjacent spins in order to transition from one macroscopic profile to the other. However, breaking so many edges simultaneously is an event with exponentially small probability.

In this note, we introduce the double flip move that introduces direct transitions between these dominant profiles. When combined with the Swendsen-Wang algorithm, it accelerates the mixing of these Ising model under the critical temperature significantly.

When the Ising model exhibits an exact symmetry (typically a reflection that negates the mixed boundary condition), the double flip move consists of

1. A geometric flip of the spin lattice along a symmetry line.
2. A spin-value flip at the interior vertices of the Ising model.

The key observation is that these two flips together preserves the alignment between the adjacent spins, hence introducing a successful Monte Carlo move. When the Ising model exhibits only an approximate symmetry, the double flip move consists of

1. A geometric flip of the spin lattice along a symmetry line.
2. A matching step that snaps the flipped copy of the interior vertices to the original copy of the interior vertices.
3. A spin-value flip at the interior vertices of the Ising model.

In both the exact and the approximate symmetry case, we prove the detailed balance of the double flip move and demonstrate its efficiency when combined with the Swendsen-Wang algorithm.

Related works. Alexander and Yoshida [1, 2] studied the spectral gap of the 2D Ising models with mixed boundary conditions. More recently, Gheissari and Lubetzky [5] studied the effect of the boundary condition for the 2D Potts models at the critical temperature. Chatterjee and Diaconis [3] showed that, for uniform equilibrium distribution, the convergence to stationarity can often be considerably speeded up by alternating every step of the Markov chain with a deterministic move.

Contents. The rest of the note is organized as follows. Section 2 reviews the Swendsen-Wang algorithm for the Ising models with boundary condition. Section 3 describes the double flip move for models with exact symmetry and Section 4 extends it to models with approximate symmetry. Section 5 discusses some future directions.

2. Swendsen-Wang Algorithm

In this section, we briefly review the Swendsen-Wang algorithm, which is a Markov Chain Monte Carlo method for sampling $p_I(\cdot)$. The description here is adapted to the setting with boundary condition. In each iteration, it generates a new configuration $(t_i)_{i \in I}$ from the current configuration $(s_i)_{i \in I}$ as follows:

1. Generate an edge configuration $w = (w_e)_{e \in E}$. For an interior edge $e = ij$, if the spin values s_i and s_j are different, set $w_{e=ij} = 0$. If s_i and s_j are the same, $w_{e=ij}$ is sampled from the Bernoulli distribution $\text{Ber}(1 - e^{-2\beta})$, i.e., equal to 1 with probability $1 - e^{-2\beta}$ and 0 with probability $e^{-2\beta}$. We also perform the same to each interior-boundary edge $e = ib$.
2. Regard all edges $e \in E$ with $w_e = 1$ as linked. Compute the connected components of the edge configuration w . For each connected component (or cluster) γ , if γ contains a boundary vertex, set $(t_i)_{i \in \gamma}$ to the spin of the boundary vertex. If not, set all the spins $(t_i)_{i \in \gamma}$ to all -1 or all $+1$ with equal probability.

The Swendsen-Wang algorithm satisfies the detailed balance, i.e.,

$$p_I(s)P_{\text{SW}}(s, t) = p_I(t)P_{\text{SW}}(t, s),$$

where $P_{\text{SW}}(s, t)$ is for the transition matrix of Swendsen-Wang. To see this, note that we can write

$$P_{\text{SW}}(s, t) = \sum_w P_w(s, t), \quad P_{\text{SW}}(t, s) = \sum_w P_w(t, s),$$

where $P_w(s, t)$ is the transition probability from s to t via a compatible edge configuration w and the sum above is taken over all compatible edge configurations w . Therefore, it is sufficient to show

$$p_I(s)P_w(s, t) = p_I(t)P_w(t, s)$$

for any compatible edge configuration w . Since the transition probability of going from the edge configuration w to the spin configurations s and t are the same, it reduces to showing

$$p_I(s)P(s, w) = p_I(t)P(t, w),$$

where $P(s, w)$ is the probability of obtaining the edge configuration w from s and similarly for $P(t, w)$. In fact $p_I(s)P(s, w)$ is independent of the spin configuration s by the following argument. First, if an interior edge $ij \in E$ has configuration $w_{ij} = 1$, then $s_i = s_j$. Second, if $ij \in E$ has configuration $w_{ij} = 0$, then s_i and s_j can either be the same or different. In the former case $s_i = s_j$, the contribution to $p_I(s)P(s, w)$ from edge ij is

$$\frac{e^\beta}{e^\beta + e^{-\beta}} \cdot e^{-2\beta} = \frac{e^{-\beta}}{e^\beta + e^{-\beta}}$$

up to a normalization constant. In the latter case $s_i = -s_j$, the contribution is also

$$\frac{e^{-\beta}}{e^\beta + e^{-\beta}} \cdot 1 = \frac{e^{-\beta}}{e^\beta + e^{-\beta}}$$

up to the same normalization constant. Second, the same argument applies to any interior-boundary edge $ib \in E$. Putting them together verifies that $p_I(s)P(s, w)$ is independent of the spin configuration s .

Another interpretation of the Swendsen-Wang algorithm is a special case of the data augmentation method [7]. To see this, one introduces the following two related probability distributions [4]: the first one is the joint vertex-edge distribution

$$\begin{aligned} p_{IE}(s, w) &\sim \prod_{ij \in E} ((1 - e^{-2\beta})\delta_{s_i=s_j}\delta_{w_{ij}=1} + e^{-2\beta}\delta_{w_{ij}=0}) \\ &\times \prod_{ib \in E} ((1 - e^{-2\beta})\delta_{s_i=f_b}\delta_{w_{ib}=1} + e^{-2\beta}\delta_{w_{ib}=0}), \end{aligned} \quad (2.1)$$

while the second one is the edge distribution

$$p_E(w) \sim \prod_{w_{ij}=1} (1 - e^{-2\beta}) \prod_{w_{ij}=0} e^{-2\beta} \cdot \prod_{w_{ib}=1} (1 - e^{-2\beta}) \prod_{w_{ib}=0} e^{-2\beta} \cdot 2^{|\mathcal{C}_w|}, \quad (2.2)$$

where \mathcal{C}_w is set of connected components of w that contain only the interior vertices. Summing $p_{IE}(s, w)$ over s or w gives

$$\sum_s p_{IE}(s, w) = p_E(w), \quad \sum_w p_{IE}(s, w) = p_I(s). \quad (2.3)$$

A direct consequence of (2.3) is that the Swendsen-Wang algorithm can be viewed as a data augmentation method [7] for sampling the joint vertex-edge distribution $p_{IE}(s, w)$, where the first substep samples the edge configuration w conditioned on the spin configuration s and the second substep samples a new spin configuration t conditioned on the edge configuration w . Once we are able to sample $p_{IE}(s, w)$, taking the marginal of the spin configuration s results in the distribution $p_I(s)$.

Though highly effective for Ising models with free boundary conditions, The Swendsen-Wang algorithm unfortunately does not encourage transitions between the dominant profiles shown in Fig. 1.1. The reason is that, for these mixed boundary condition, such a transition requires breaking a macroscopic number of edges between aligned adjacent spins, which has an exponentially small probability. This is the motivation for introducing the double flip move.

3. Double Flip for Symmetric Models

The double flip move is designed to introduce explicit transitions between the macroscopic profiles as shown Fig. 1.1. This section assumes that the Ising model enjoys an explicit graph involution, i.e., there exists a map $m : V \rightarrow V$ such that:

- m maps I to I and B to B , respectively, and $m^2 = \text{id}$,
- $ij \in E$ iff $m(i) \sim m(j) \in E$, and $ib \in E$ iff $m(i)m(b) \in E$,
- $f_{m(b)} = -f_b$.

For example, in Fig. 1.1(a) m is the reflection along one of the diagonals of the square, while in Fig. 1.1(b) m is the reflection along the x axis.

In the double flip move, the first flip implements the map m to the interior vertices in I . After that, the second flip negates the spin of the mapped interior vertices. More specifically, the resulting new spin configuration t is defined by

$$t_{m(i)} = -s_i, \quad \forall i \in I. \quad (3.1)$$

Since $m^2 = \text{id}$, we also have $t_i = -s_{m(i)}$ for any $i \in I$.

Theorem 3.1. *The double flip move satisfies the detailed balance.*

Proof. To show the detailed balance, one needs to prove that, for any two spin configurations s and t ,

$$p_I(s)P_{\text{DF}}(s, t) = p_I(t)P_{\text{DF}}(t, s),$$

where P_{DF} is the double flip move transition matrix. From the definition of the double flip move, the transition probabilities $P(s, t)$ and $P(t, s)$ equal to one if s and t satisfy (3.1) and zero otherwise. Hence, it is sufficient to show $p_I(s) = p_I(t)$ when (3.1) holds.

For each $ij \in E$,

$$t_i t_j = (-1)^2 s_{m(i)} s_{m(j)} = s_{m(i)} s_{m(j)}.$$

Taking the sum over all interior edges gives

$$\sum_{ij \in E} t_i t_j = \sum_{ij \in E} s_{m(i)} s_{m(j)} = \sum_{ij \in E} s_i s_j.$$

For each $ib \in E$,

$$t_i f_b = (-1)^2 s_{m(i)} f_{m(b)} = s_{m(i)} f_{m(b)}.$$

Taking the sum over all interior edges results in

$$\sum_{ib \in E} t_i f_b = \sum_{ib \in E} s_{m(i)} f_{m(b)} = \sum_{ib \in E} s_i f_b.$$

Together,

$$\sum_{ij \in E} t_i t_j + \sum_{ib \in E} t_i f_b = \sum_{ij \in E} s_i s_j + \sum_{ib \in E} s_i f_b,$$

i.e., $p_I(s) = p_I(t)$.

We can now combine the double flip move with the Swendsen-Wang move. For a constant $\eta \in (0, 1)$, each iteration of the combined algorithm performs the double flip move with probability η and the Swendsen-Wang move with probability $1 - \eta$:

1. Choose u from $\text{Ber}(\eta)$, i.e., equal to 1 with probability η .
2. If u is 1, perform the double flip move, else perform the Swendsen-Wang move.

Theorem 3.2. *The Swendsen-Wang algorithm with double flip satisfies the detailed balance.*

Proof. The combined transition matrix is

$$P_{\text{SWDF}} = \eta P_{\text{DF}} + (1 - \eta) P_{\text{SW}}.$$

Section 2 shows that the Swendsen-Wang algorithm satisfies the detailed balance, i.e.,

$$p_I(s) P_{\text{SW}}(s, t) = p_I(t) P_{\text{SW}}(t, s).$$

The double flip move satisfies the detailed balance as shown above,

$$p_I(s) P_{\text{DF}}(s, t) = p_I(t) P_{\text{DF}}(t, s).$$

A linear combination of these two statements give

$$p_I(s) P_{\text{SWDF}}(s, t) = p_I(t) P_{\text{SWDF}}(t, s)$$

and this finishes the proof.

Below we compare the performance of the Swendsen-Wang algorithm (SW) and Swendsen-Wang with double flip (SWDF) using two examples.

Example 3.1. The Ising model is a square lattice. The mixed boundary condition is +1 at the two vertical sides and -1 at the two horizontal sides. The graph involution $m : V \rightarrow V$ is given by the diagonal reflection. Fig. 3.1(a) shows the model at size $n_1 = n_2 = 20$. Fig. 3.1(b) gives the two dominant macroscopic profiles.

The experiments are performed for the problem size $n_1 = n_2 = 100$ at the inverse temperature $\beta = 0.5$. We start from the all -1 configuration and carry out 10000 iterations for both SW and SWDF. For SWDF, we set the parameter $\eta = 1/100$. Figs. 3.1(c)-(d) plot the average spin value

$$\frac{1}{|I|} \sum_{i \in I} s_i$$

of these two algorithms, respectively. Fig. 3.1(c) shows that SW fails to introduce transitions between the -1 and the +1 macroscopic profiles, since the average spin always stays below 0. On the other hand, Fig. 3.1(d) demonstrates that SWDF explores both profiles with about 100 transitions in between.

We further conduct a comparison between SW and SWDF around β_c , the critical inverse temperature. Fig. 3.2 plots the behavior of SW (left) and SWDF (right) for three β values near

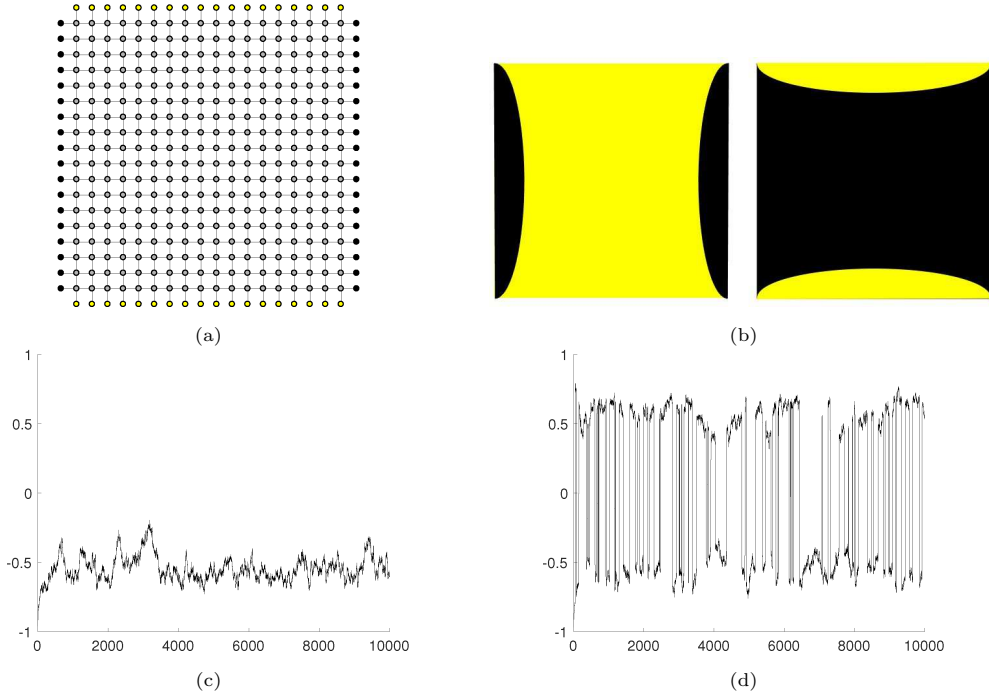


Fig. 3.1. (a) The lattice along with the mixed boundary condition (black for $+1$ and yellow for -1). (b) Two dominant macroscopic profiles. (c) The average spin value of the Swendsen-Wang algorithm. (d) The average spin value of the Swendsen-Wang algorithm with double flip.

the critical temperature: $\beta = 0.45, 0.46, 0.47$ from top to bottom. For each case, the plot gives the average spin value over the iterations. These plots clearly show that SW explores the spin configurations effectively when $\beta < \beta_c$ but fails when $\beta > \beta_c$. On the other hand, SWDF is able to explore the whole spin configuration space effectively, uniformly across β_c .

Example 3.2. The Ising lattice is still a square. The mixed boundary condition is $+1$ in the first and third quadrants but -1 in the second and fourth quadrants. The graph involution $m : V \rightarrow V$ is given by the reflection along either the x or the y axis. Fig. 3.3(a) shows the problem at size $n_1 = n_2 = 20$. Fig. 3.3(b) gives the two dominant macroscopic profiles.

Similar to the previous example, the experiments are performed for the problem size $n_1 = n_2 = 100$ at the inverse temperature $\beta = 0.5$. We start from the all -1 configuration and carry out 10000 iterations for both SW and SWDF. The η parameter of SWDF is $1/100$. Fig. 3.3(c) shows that SW fails to introduce transitions between the -1 dominant and the $+1$ dominant macroscopic profiles, while Fig. 3.3(d) demonstrates that SWDF explores both profiles with about 100 transitions in between.

4. Double Flip for Approximately Symmetric Models

The algorithm in Section 3 is efficient but depends on exact symmetries. However, many Ising models without exact symmetries also exhibit different macroscopic profiles such as in Fig. 1.1(b). This section extends the double flip move to models with approximate symmetry.

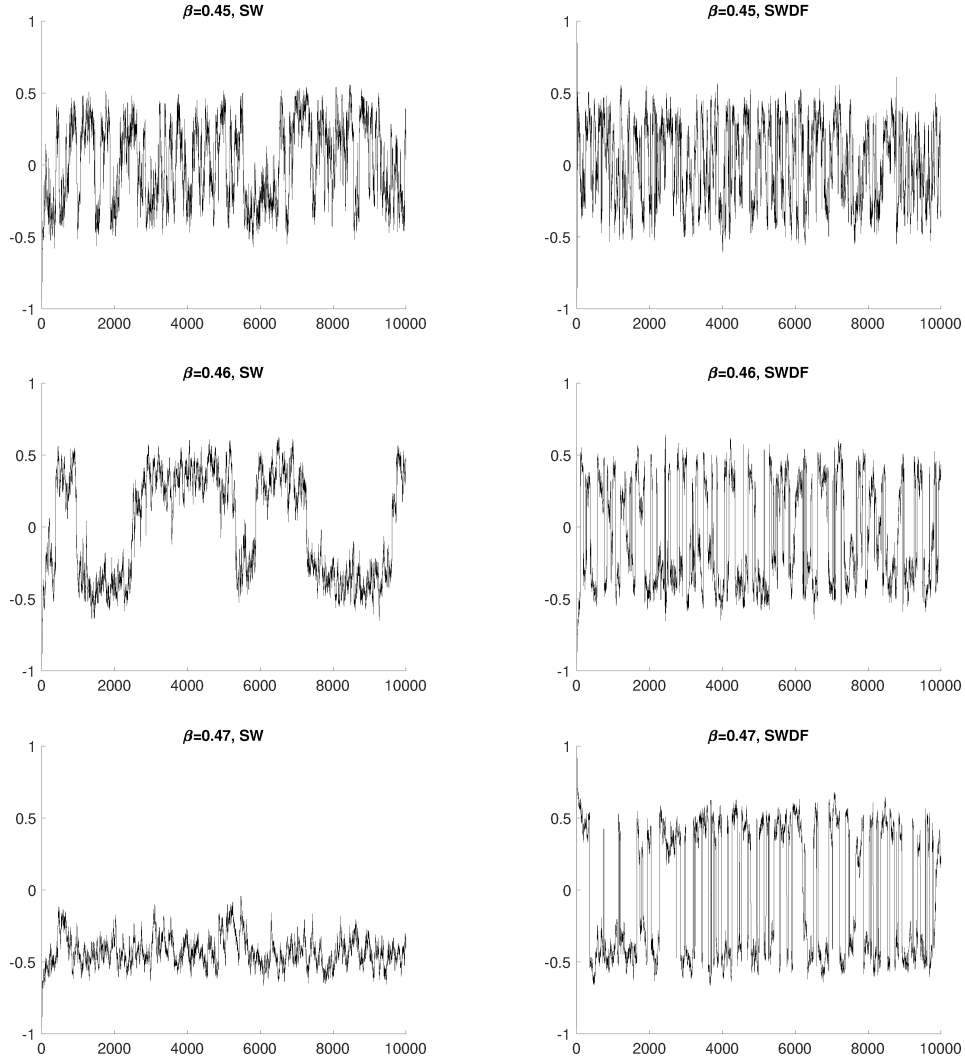


Fig. 3.2. The comparison of Swendsen-Wang (SW) and Swendsen-Wang with double flip (SWDF) near the critical temperature. From top to bottom: $\beta = 0.45, 0.46, 0.47$ and therefore the physical temperature decreases. From left to right: SW and SWDF.

Here we take a more geometric viewpoint and assume that the Ising model is embedded in a domain $\Omega \subset \mathbb{R}^2$ with the boundary denoted by $\partial\Omega$.

- For each $i \in I$, x_i is in the interior of Ω . For each $b \in B$, x_b is in $\partial\Omega$.
- The edges ij (interior) and ib (interior-boundary) in the set E are segments between geometrically nearby vertices.
- $\partial\Omega = \partial\Omega_+ \cup \partial\Omega_-$.

$$f_b = \begin{cases} 1, & \text{if } x_b \in \partial\Omega_+, \\ -1, & \text{if } x_b \in \partial\Omega_-. \end{cases}$$

- Assume that there is a continuous involution $\mu : \bar{\Omega} \rightarrow \bar{\Omega}$ such that $\mu^2 = \text{id}$, $\mu(\partial\Omega_+) = \partial\Omega_-$.

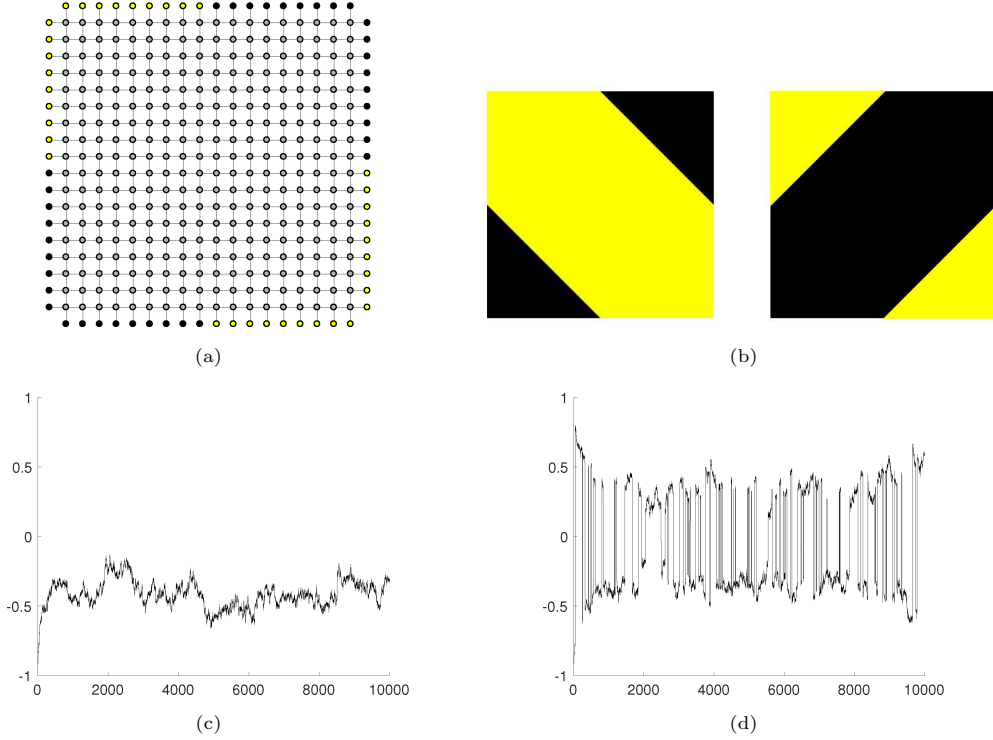


Fig. 3.3. (a) The lattice along with the mixed boundary condition (black for $+1$ and yellow for -1). (b) The average spin value of the Swendsen-Wang algorithm. (c) The average spin value of the Swendsen-Wang algorithm with double flip.

Since μ is only defined as an involution of Ω , in general $\{\mu(x_i)\}_{i \in I} \neq \{x_i\}_{j \in I}$ and therefore μ does not directly introduce an involution on the set I of interior vertices. To fix this, we introduce a discrete involution $m : I \rightarrow I$ such that

$$x_{m(i)} \approx \mu(x_i). \quad (4.1)$$

We shall discuss below how to construct m based on μ . For now, we assume the existence of m and define a Metropolized double flip move for approximately symmetric models.

1. Define a spin configuration t via $t_i = -s_{m(i)}$.
2. Evaluate $c = \min(1, p_I(t)/p_I(s))$.
3. Sample $u \in [0, 1]$ uniformly. If $u \leq c$, set t to be the new spin configuration. Otherwise, keep s as the spin configuration.

Since m is an involution and this is a Metropolized move, the following statement holds.

Theorem 4.1. *The Metropolized double flip move satisfies the detailed balance.*

It can also be combined with the Swendsen-Wang move in the same way as described in Section 3.

Theorem 4.2. *The Swendsen-Wang algorithm with Metropolized double flip satisfies the detailed balance.*

The efficiency of this algorithm depends on the condition that $p_I(t)/p_I(s)$ is neither too small or too large. This is in fact promoted by the condition (4.1), since $ij \in E$ would imply

$$x_{m(i)} \approx \mu(x_i) \approx \mu(x_j) \approx x_{m(j)},$$

where the second step uses the continuity of the domain involution μ . Therefore, when $ij \in E$, $m(i)m(j)$ is also likely to be an edge of E and in particular

$$s_i s_j = (-1)^2 s_i s_j = t_{m(i)} t_{m(j)}.$$

If this holds for most pairs $ij \in E$ and $ib \in E$, $p_I(t)/p_I(s)$ is likely to be well-bounded away from both zero and infinity.

The remaining question is how to construct $m : I \rightarrow I$ so that $m^2 = \text{id}$ and (4.1) holds. One possibility is to formulate this as a matching problem between the geometrically flipped vertices $\{\mu(x_i)\}_{i \in I}$ and the original vertices $\{x_j\}_{j \in I}$, with a cost defined using either the ℓ_2 or the ℓ_∞ distance. Equivalently, this can be viewed as an optimal transport problem between the two distributions

$$\sum_{i \in I} \delta_{\mu(x_i)}(\cdot) \quad \text{and} \quad \sum_{j \in I} \delta_{x_j}(\cdot).$$

Once the matching (or the transport map) is available, we define $m(i) = j$ if $\mu(x_i)$ is matched with x_j . However, this approach has two technical difficulties:

- The computation cost of the matching or optimal transport algorithm [6, 8] can be relatively high.
- The involution condition $m^2 = \text{id}$ is not guaranteed.

In the implementation, we adopt the following heuristic procedure. Assume without loss of generality that the domain Ω is centered at the origin.

1. Order the interior vertices $\{x_j\}_{j \in I}$ based on their distances to the origin in the decreasing order. The distance is typically chosen to be either the ℓ_∞ norm or the ℓ_2 norm.
2. Mark all vertices $j \in I$ as unpaired.
3. Scan the interior vertices in this ordered list. For each x_j , if j is already paired, then skip. If not, find the unpaired i such that $\mu(x_i)$ is closet to x_j , pair i and j

$$m(i) := j, \quad m(j) := i,$$

and mark both i and j as paired.

The heuristic is that, by following the order of decreasing distance to the origin, the remaining unpaired vertices are forced to cluster near the center of the domain, thus reducing the overall transport cost.

Below we compare the performance of the Swendsen-Wang algorithm (SW) and Swendsen-Wang with Metropolized double flip (SWDF) using three examples.

Example 4.1. The Ising model is a rectangular lattice where the number of rows and columns are different, as shown in Fig. 4.1. The mixed boundary condition is $+1$ at the two vertical sides and -1 at the two horizontal sides. The diagonal reflection is no longer an exact symmetry.

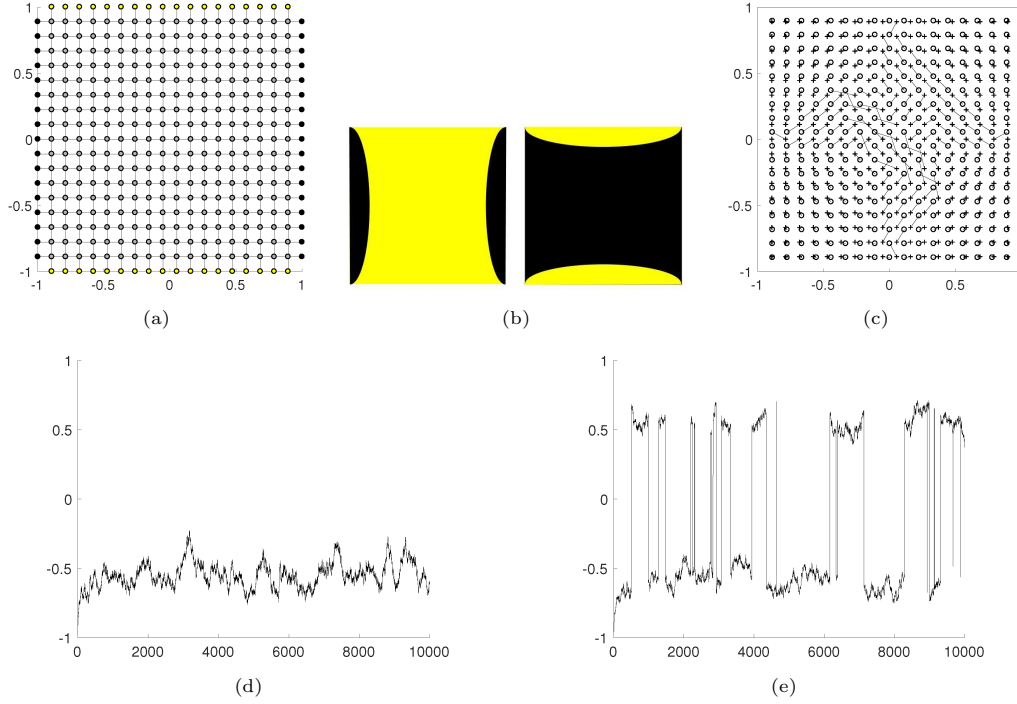


Fig. 4.1. (a) The rectangular lattice along with the mixed boundary condition (black for $+1$ and yellow for -1). (b) Two dominant macroscopic profiles. (c) The transport map from $\{\mu(x_i)\}_{i \in I}$ (marked with $+$) to $\{x_j\}_{j \in I}$ (marked with \circ). (d) The average spin value of the Swendsen-Wang algorithm. (e) The average spin value of the Swendsen-Wang algorithm with double flip.

Fig. 4.1(a) shows the system with size 20×19 . Fig. 4.1(b) gives the two dominant macroscopic profiles. Fig. 4.1(c) plots the transport map between $\{\mu(x_i)\}_{i \in I}$ (marked with $+$) to $\{x_j\}_{j \in I}$ (marked with \circ). As shown, the transport map is quite local, demonstrating the efficiency of the heuristic matching procedure.

The experiments are performed for the problem size 100×99 at the inverse temperature $\beta = 0.5$. We start from the all -1 configuration and carry out 10000 iterations for both SW and SWDF. The η parameter of SWDF is $\eta = 1/3$. Fig. 4.1(d) shows that SW fails to introduce transitions between the -1 dominant and the $+1$ dominant macroscopic profiles, while Fig. 4.1(e) demonstrates that SWDF explores both profiles with 41 transitions out of about 3000 trials.

Example 4.2. The Ising model is a random quasi-uniform triangular lattice supported on the unit disk, as shown in Fig. 4.2. The mixed boundary condition is equal to $+1$ in the first and third quadrants but -1 in the second and fourth quadrants. The problem does not have strict rotation and reflection symmetry due to the random triangulation. Fig. 4.2(a) shows the triangulation with mesh size $h = 0.1$. Fig. 4.2(b) gives the two dominant macroscopic profiles. Fig. 4.2(c) gives the transport map between $\{\mu(x_i)\}_{i \in I}$ (marked with $+$) to $\{x_j\}_{j \in I}$ (marked with \circ), which is quite local.

The experiments are performed with a finer triangulation with mesh size $h = 0.05$ at the inverse temperature $\beta = 0.5$. We start from the all -1 configuration and carry out 10000 iterations for both SW and SWDF. The η parameter of SWDF is $1/3$. Fig. 4.2(d) shows that

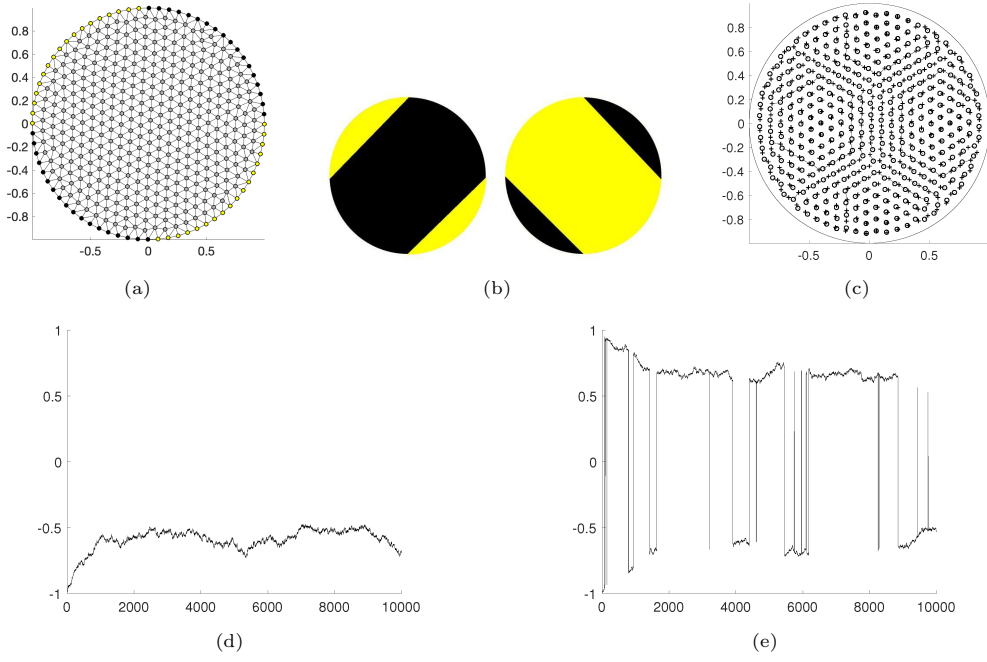


Fig. 4.2. (a) The lattice along with the mixed boundary condition (black for $+1$ and yellow for -1). (b) Two dominant macroscopic profiles. (c) The transport map from $\{\mu(x_i)\}_{i \in I}$ (marked with $+$) to $\{x_j\}_{j \in I}$ (marked with \circ). (d) The average spin value of the Swendsen-Wang algorithm. (e) The average spin value of the Swendsen-Wang algorithm with double flip.

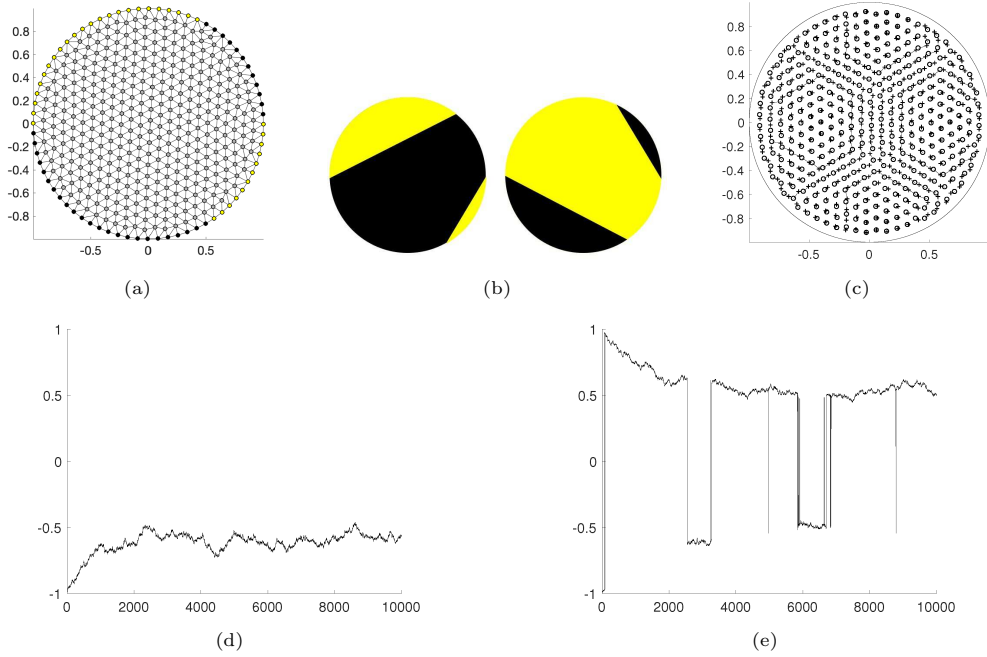


Fig. 4.3. (a) The lattice along with the mixed boundary condition (black for $+1$ and yellow for -1). (b) Two dominant macroscopic profiles. (c) The transport map from $\{\mu(x_i)\}_{i \in I}$ (marked with $+$) to $\{x_j\}_{j \in I}$ (marked with \circ). (d) The average spin value of the Swendsen-Wang algorithm. (e) The average spin value of the Swendsen-Wang algorithm with double flip.

SW fails to introduce transitions between the -1 dominant and the $+1$ dominant macroscopic profiles, while Fig. 4.2(e) demonstrates that SWDF explores both profiles with 48 transitions out of about 3000 trials.

Example 4.3. The Ising model is again a random quasi-uniform triangular lattice supported on the unit disk. The mixed boundary condition is equal to $+1$ on the two arcs with angle in $[0, \pi/3]$ and $[\pi, 5\pi/3]$ and -1 on the remaining two arcs. Due to the random triangulation, the problem does not have strict rotation and reflection symmetry. Fig. 4.3(a) shows the triangulation with mesh size $h = 0.1$. Fig. 4.3(b) gives the two dominant macroscopic profiles. Fig. 4.3(c) plots the transport map between $\{\mu(x_i)\}_{i \in I}$ (marked with $+$) to $\{x_j\}_{j \in I}$ (marked with \circ).

The experiments are performed with a finer triangulation with mesh size $h = 0.05$ at the inverse temperature $\beta = 0.5$. We start from the all -1 configuration and carry out 10000 iterations for both SW and SWDF. The η parameter of SWDF is $\eta = 1/3$. Fig. 4.3(d) shows that SW fails to introduce transitions between the -1 dominant and the $+1$ dominant macroscopic profiles, while Fig. 4.3(e) demonstrates that SWDF explores both profiles with 35 transitions out of about 3000 trials.

5. Discussions

This note introduces the double flip move for accelerating the Swendsen-Wang algorithm for Ising models with mixed boundary conditions. We consider both symmetric and approximately symmetric models. In both cases, we prove the detailed balance and demonstrated its efficiency in introducing explicit transitions between different dominant profiles.

There are many unanswered questions. Regarding the symmetric models, one question is to prove a polynomial mixing time for the examples in Section 3. Regarding the approximately symmetric models, there are more open questions:

- Is there a fast matching or optimal transport algorithm that ensures $m^2 = \text{id}$?
- Better heuristic procedures to construct a matching between $\{\mu(x_i)\}_{i \in I}$ and $\{x_j\}_{j \in I}$?
- Can we bound the acceptance ratio of the Metropolized double flip move under certain assumptions of the approximate symmetry?
- Proving a rapid mixing result for any approximately symmetric model in Section 4.
- The approximate matching is carried out for the interior vertices in this note. However, it can be carried out for the edges alternatively.

Acknowledgments. The author thanks Sourav Chatterjee for discussions and for introducing [3]. The author also thanks the reviewers for constructive comments.

This work is partially supported by NSF Grant DMS 2011699.

References

- [1] K.S. Alexander, The spectral gap of the 2-D stochastic Ising model with nearly single-spin boundary conditions, *J. Stat. Phys.*, **104** (2001), 59–87.

- [2] K.S. Alexander and N. Yoshida, The spectral gap of the 2-D stochastic Ising model with mixed boundary conditions, *J. Stat. Phys.*, **104** (2001), 89–109.
- [3] S. Chatterjee and P. Diaconis, Speeding up Markov chains with deterministic jumps, *Probab. Theory Related Fields*, **178**:3 (2020), 1193–1214.
- [4] R.G. Edwards and A.D. Sokal, Generalization of the Fortuin-Kasteleyn-Swendsen-Wang representation and Monte Carlo algorithm, *Phys. Rev. D*, **38**:6 (1988), 2009.
- [5] R. Gheissari and E. Lubetzky, The effect of boundary conditions on mixing of 2D Potts models at discontinuous phase transitions, *Electron. J. Probab.*, **23** (2018), 1–30.
- [6] H.W. Kuhn, The Hungarian method for the assignment problem, *Nav. Res. Logist.*, **2**:1-2 (1955), 83–97.
- [7] J.S. Liu, *Monte Carlo Strategies in Scientific Computing*, Springer, 2001.
- [8] G. Peyré and M. Cuturi, Computational optimal transport: With applications to data science, *Found. Trends Mach. Learn.*, **11**:5-6 (2019), 355–607.
- [9] R.H. Swendsen and J.S. Wang, Nonuniversal critical dynamics in Monte Carlo simulations, *Phys. Rev. Lett.*, **58**:2 (1987), 86.